Article

Adsorptive and Surface Characterization of Mediterranean Agrifood Processing Wastes: Prospection for Pesticide Removal

José A. Fernández-López [1],*, Marta Doval Miñarro [1], José M. Angosto [1], Javier Fernández-Lledó [2] and José M. Obón [1]

1 Department of Chemical and Environmental Engineering, Technical University of Cartagena (UPCT), Paseo Alfonso XIII, 52 E-30203 Cartagena, Murcia, Spain; marta.doval@upct.es (M.D.M.); jm.angosto@upct.es (J.M.A.); josemaria.obon@upct.es (J.M.O.)
2 Higher Technical School of Industrial Engineering, Technical University of Cartagena (UPCT), Campus Muralla del Mar, E-30202 Cartagena, Murcia, Spain; javier.fernandezl@edu.upct.es
* Correspondence: josea.fernandez@upct.es; Tel.: +34-968325549

Abstract: The sustainable management of biomass is a key global challenge that demands compliance with fundamental requirements of social and environmental responsibility and economic effectiveness. Strategies for the valorization of waste biomass from agrifood industries must be in line with sustainable technological management and eco-industrial approaches. The efficient bioremoval of the pesticides imazalil and thiabendazole from aqueous effluents using waste biomass from typically Mediterranean agrifood industries (citrus waste, artichoke agrowaste and olive mill residue) revealed that these residues may be transformed into cost-effective biosorbents. Agrifood wastes present irregular surfaces, many different sized pores and active functional groups on their surface, and they are abundant in nature. The surface and adsorptive properties of olive mill residue, artichoke agrowaste and citrus waste were characterized with respect to elemental composition, microstructure, crystallinity, pore size, presence of active functional groups, thermal stability, and point of zero charge. Olive mill residue showed the highest values of surface area (Brunauer–Emmett–Teller method), porosity, crystallinity index, and pH of zero point of charge. Olive mill residue showed the highest efficiency with sorption capacities of 9 mg·g^{-1} for imazalil and 8.6 mg·g^{-1} for thiabendazole.

Keywords: agrifood waste; plant biomass; adsorption; bioremoval; water pollutants

1. Introduction

The 2030 Agenda for Sustainable Development adopted by all United Nations member countries in 2015 stated a shared blueprint for our planet [1,2]. This document set 17 sustainable development goals, of which the sustainable use of ecosystems and the improvement of water quality by reducing pollution were particularly highlighted [3]. At this point, it should be stressed that appropriate steps need to be taken to enhance the value of the wastes generated by the agrifood sector.

Water pollution causes human health problems, wildlife poisoning, and long-term damage to ecosystems. It has become a major global challenge that requires ongoing evaluation and effective remediation technologies [4]. Water bodies can be polluted by a wide variety of substances, including toxic chemicals, plant nutrients, organic wastes, medicines, and pathogenic microorganisms. Different treatment processes are applied to remove these pollutants from wastewaters, including membrane filtration, photodegradation, ion exchange, electrochemical treatment, chemical oxidation or reduction, and sorption [5].

Adsorption is a proven and effective alternative technology for the removal of pollutants from aqueous effluent [6,7]. Multiple sorbents have been successfully tested, and numerous research and review papers have been published in this field [8–10]. Agrifood wastes, industrial byproducts, and biochars are considered to be efficient eco-friendly sorbents with potential use for environmental applications [11–13].

Biomass can be defined in broad terms as any organic matter derived from biogenic sources that are available on a renewable basis [14]. Wood, forest residue, grass, energy crops, and agrifood residue are all types of lignocellulosic biomass [15].

Large amounts of agrifood waste are produced throughout the supply chain, from initial production stages to final consumption. The global annual production of lignocellulosic biomass including agrifood waste and greenhouse biomass is estimated at around 200 billion tonnes [16]. Artichoke agrowaste and citrus waste residues are partially used as a source of bioactive compounds [17,18] although mostly they are discarded as green manure or used in livestock feed [19]. Olive mill residue constitutes a promising biomass resource, being mainly used for energy purposes because of their thermochemical characteristics [20]. However, modern green technologies are available that make it possible to efficiently use this waste biomass of the agrifood industries to produce value-added products such as commodity chemicals (biofuels), highly effective carbonaceous sorbents, or even bioactive compounds for the food or pharmaceutical industries [18,21].

Lignocellulosic biomass is highlighted prominently as a sustainable alternative to fossil carbon resources in the production of second-generation biofuels and other bio-based chemicals [22,23]. Alternatively, a significant number of studies have reported the feasibility of transforming lignocellulosic biomass into valuable sorbent material which improves and upgrades the bioremoval of contaminants in aqueous effluent [24–26]. Lignocellulose is a three-dimensional nanocomposite consisting of a dynamic mixture of multifunctional constituents. The major components of lignocellulosic biomass are cellulose (30–35%), hemicellulose (20–40%), and lignin (15–25%) [27]. Cellulose is a linear polymer of β-1,4-linked glucose residues and is the main component of plant cell walls [28]. Hemicellulose is composed of heteropolymers and is derived from a miscellaneous group of sugars (including d-xylose, d-galactose, and d-mannose) and sugar acids (d-glucuronic and d-galacturonic acids). The presence of a different number of sugar units in the hemicellulose side chains results in different three-dimensional structures of the hemicellulose molecules that confer relevant adsorptive properties. In addition, hemicelluloses may contain slightly ionized organic acids in their side chains, which increase the adsorption capacity of the biomass [29]. Lignin is an amorphous aromatic biopolymer of propyl phenol units, namely, sinapyl alcohol, coniferyl, and a minor quantity of *p*-coumaryl alcohol. In plants, lignin surrounds the cellulose microfibrils and strengthens the cell walls [30]. Lignin is difficult to decompose due to its high degree of cross-linkages, and moreover, it is characterized by an abundance of electron-donor active sites which are provided in the polyphenol and polyhydroxy functional groups, offering an exceptional frame for the binding and interaction with cationic pollutants [31].

Citrus fruits, olives, and artichokes are typical crops in the Mediterranean basin. The industrial processing of these crops generates vast quantities of agrifood residue. The citrus processing industries produce solid waste consisting of pulp, peels, and whole fruits that do not meet quality criteria [32]. Olive mill waste biomass is the solid residue of olive oil factories. This residue is mostly composed of olive pulp and stones [33]. The industrial processing of the artichokes produces a solid residue composed essentially by the external bracts and stems of the flowers, which constitutes about 70–80% of the total artichoke flower [34].

These agrifood residues are poorly managed and rarely exploited, although there is no doubt that many greater benefits could be obtained from these materials through a more detailed knowledge of their physicochemical properties. In order to contribute more actively to the development of a circular economy, there is a growing interest in the scientific community to provide sustainable solutions for the valorization of these agrifood wastes.

According to reported studies, municipal wastewater is considered the main source of pesticide emissions into the environment [35,36]. After the use of products containing pesticides, a mass of them is discharged into the wastewater and reaches the wastewater treatment plants through the sewage system. In general, pesticides cannot be completely

eliminated from these plants using conventional treatment technologies, which undoubtedly represents a potential ecological risk, because while these substances do not generally pose acute risks to aquatic organisms or humans, their long-term effects and especially their potential synergistic impacts are still unknown in most cases. Imazalil (IMZ) and thiabendazole (TBZ) are systemic fungicides employed to control a wide range of fungal diseases on fruit, greens, and ornamentals. Both fungicides are most widely used in packinghouse treatments to control postharvest decay in citrus and banana fruits. TBZ is also painted onto housing materials as an antifungal agent, and is used in clothing manufacture as antifungal processing agent.

The main objective of this work was to characterize the physicochemical properties of the agrifood biomass resulting from the industrial processing of citrus fruits, olives, and artichokes, in order to obtain new data on the relationship between adsorptive parameters (composition, microstructure, crystallinity, pore size, presence of active functional groups on the surface, thermal stability, and the point of zero charge) and bioremoval capacity with respect to emergent water pollutants such as imazalil or thiabendazole.

2. Materials and Methods

2.1. Conditioning of Agrifood Wastes

The agrifood wastes selected included solid residues from the citrus processing industry (rejected fruit, pulp portions, peels, and seeds), the olive oil industry (olive pulp and stones after mechanical and water extraction of the oil content), and the artichoke canning industry (external bracts and stems of the flowers). All these factories were located in the region of Murcia (Spain). All agrifood residue was washed repeatedly with water to remove dust and soluble impurities, then oven-dried at 60 °C to constant weight. The dried biomass was ground in a laboratory knife mill to pass through an 18-mesh sieve (1.00 mm). The sorbent powders obtained were then stored at room temperature prior to use.

2.2. Agrifood Waste Biomass Characterization

The elemental analysis of the agrifood waste biomass was carried out using a 628 Series Leco CHNS/O Analyzer (Leco Corp., St. Joseph, MI, USA). The higher heating values (HHV) of the biomass were calculated using the Channiwala and Parikh equation [37]:

$$\text{HHV (MJ/kg)} = 0.3491C + 1.1783H + 0.1005S - 0.1034O - 0.0151N - 0.0211A \qquad (1)$$

where C, H, S, O, N, and A represent carbon, hydrogen, sulfur, oxygen, nitrogen, and ash content of biomass, respectively, expressed in mass percentages on a dry basis.

The surface chemistry of the sorbents was characterized using scanning electron microscopy (SEM) and Fourier-transform infrared spectroscopy (FTIR). The surface microstructure was analyzed using a Hitachi S-3500 N electron microscope (Hitachi Ltd., Krefeld, Germany). SEM images were obtained at 15 kV with a working distance of 17 mm and different magnifications. Biomass samples were scattered on double-sided tape and mounted over an aluminum sample holder.

Infrared spectra were recorded at room temperature to identify the functional groups present on the surface of the sorbents. A Thermo Nicolet 5700 (ThermoFisher Scientific, Karlsruhe, Germany) was used, in the range of 4000 to 400 cm^{-1} and in transmittance mode.

X-ray diffraction (XRD) was used to analyze the crystallinity of the sorbents. The diffractograms were recorded using an XRD Bruker D8 Advance instrument (Bruker corp., Karlsruhe, Germany) with Cu Kα radiation, a voltage of 40 kV, and a current of 20 mA. The scanning range was from $2\Theta = 5°$ to $50°$ at a scan speed of $0.05°\cdot\text{s}^{-1}$.

Thermogravimetric analysis was performed using a TGA/DSC 1 HT instrument (Mettler-Toledo GmbH, Giessen, Germany), operating in a nitrogen atmosphere. Mass samples of 9–11 mg were taken into a ceramic crucible and heated up from 25 to 900 °C at 10 °C/min under static conditions.

The specific surface area and the pore size distribution of the powder sorbents were measured using N$_2$ and CO$_2$ gas sorption and Hg porosimetry, respectively. Sorption–

desorption isotherms of N_2 at $-196\ ^\circ\text{C}$ were determined using an Autosorb iQ XR-2 automated gas sorption analyzer (Quantachrome Instruments, Boynton Beach, Florida). Prior to the gas sorption measurements, the samples were degassed at $100\ ^\circ\text{C}$ for 24 h. The surface area and pore volumes were determined using the standard Brunauer–Emmett–Teller (BET) method [38]. In parallel, a surface analysis was also conducted, using CO_2 gas as the adsorbate to quantify the narrow micropores (<1 nm). A PoreMaster 60-GT porosimeter (Quantachrome Instruments, Boynton Beach, FL, USA), was used to analyze the pore size distribution of the raw sorbents. Prior to the analysis, the samples were degassed at $100\ ^\circ\text{C}$ for 24 h. The density of the samples was calculated using helium pycnometry with an UltraPyc gas pycnometer (Quantachrome Instruments, Boynton Beach, FL, USA).

The zero points of charge (pH_{ZPC}) of the agrowaste sorbents were determined using the mass titration method [39]. The method consists of putting different samples of sorbent into contact with a 0.03 M KNO_3 solution within a dosage range of 5–100 g/L. These suspensions were stirred for 24 h at 150 rpm until the equilibrium pH was reached. The pH_{ZPC} was determined as the pH at which a plateau was reached when plotting equilibrium pH vs. sorbent dosage.

2.3. Imazalil and Thiabendazole Batch Sorption Experiments

A weighed quantity of imazalil [$C_{14}H_{14}Cl_2N_2O$; 1-[2-(allyloxy)-2-(2,4-dichlorophenyl)-ethyl]imidazole] or thiabendazole [$C_{10}H_7N_3S$; 2-(4-thiazolyl)benzimidazole] was dissolved in deionized water in order to prepare the 50 or 150 mg/L solutions, respectively. Further concentrations were achieved by dilution in deionized water. For the sorption experiments, working solutions of IMZ and TBZ (10 mg/L) were made from the stock solutions. Batch experiments were performed at room temperature ($22\ ^\circ\text{C}$) under agitation in a reciprocal shaker by contact with 100 mL of the fungicide working solution at a fixed concentration and a known quantity of sorbent biomass (0.1 g) for 24 h in a conical flask at a constant agitation speed of 150 rpm, in dark conditions. The solutions were then filtered through a 0.45 μm pore size nylon membrane filter and the residual fungicide concentrations in the filtrate were quantified through high-performance liquid chromatography (HPLC) [40] in a Waters instrument (Waters Chromatography Europe BV, Etten-Leur, The Netherlands). A Symmetry C18, 5 μm column (4.6 × 150 mm i.d.) containing acetonitrile—0.1% phosphoric acid in the ratio of 50:50 was used as the mobile phase (in the rate of 0.6 mL/min). Detection was performed with a photodiode array detector at 204 nm (IMZ) and 254 nm (TBZ).

The mass balance equation was used for determining the sorption capacity q_e (mg/g) of each sorbent according to the expression:

$$q_e = \frac{C_0 - C_e}{m} \cdot V \qquad (2)$$

where C_0 (mg/L) is the initial fungicide concentration, C_e (mg/L) is the equilibrium concentration after the adsorption has taken place, V is the solution volume (L), and m is the dried sorbent biomass (g) added.

For the desorption experiments, 0.1 M NaOH was used as an eluent reagent. The desorption efficiencies were determined using loaded sorbent dosages of 2.0 g/L and a stirring contact time of 6 h.

3. Results and Discussion

3.1. Elemental Analysis of the Agrifood Wastes

The elemental composition of the selected agrifood wastes on a dry weight (%) basis (Table 1), determined by means of a CHONS analyzer, revealed that C and O were, as expected [41], the predominant elements, with H, N, and S being in substantially lower proportion. A significant quantity of oxygen was revealed in these residues (46.9–49.9%), which indicated the presence of oxygen-functional groups (O−H, C−O, C=O) within them.

Functional groups with nitrogen (C−N, C≡N, N−H) and sulfur (C−S, S-H) were also present, although in a considerably smaller proportion.

Table 1. Ultimate analysis (wt, %, db) of selected agrifood wastes.

	Olive Mill Residue	Artichoke Agrowaste	Citrus Waste
C	47.0 ± 1.0 *	42.3 ± 0.9	41.3 ± 0.7
O	46.2 ± 1.9	48.1 ± 1.7	49.9 ± 2.2
H	5.2 ± 0.8	6.2 ± 0.5	5.8 ± 0.5
N	1.1 ± 0.5	3.0 ± 0.3	2.0 ± 0.4
S	0.4 ± 0.2	0.3 ± 0.1	0.9 ± 0.2
Ash	0.7 ± 0.2	5.3 ± 0.8	8.9 ± 1.2
O/C	0.98	1.14	1.21
HHV [†] (MJ/kg)	17.77	16.97	15.96

* mean $\pm$ SD of 3 determinations; [†] Higher heating value (Channiwala and Parikh [36]).

The ratio of the atomic oxygen to carbon content (O/C) is directly correlated with the energy content of a biomass. Typically, a greater presence of oxygen decreases its energy potential [42]. As a result, a higher O/C ratio in biomass reduces the energy content. In this context, the olive mill residue was that with the highest energy potential among the selected agrifood wastes. These results were confirmed after the application of the Channiwala and Parikh equation [37] to estimate the higher heating value (HHV) of the biomass samples, ranging from 17.2 MJ/kg (olive mill residue) to 15.9 MJ/kg (citrus waste).

3.2. Scanning Electron Microscopy

Scanning electron microscopy (SEM) is among the most powerful tools widely used to investigate biomass surfaces [43]. The microstructural features of the different sorbent powders were investigated by means of SEM (Figure 1). Observations carried out on a number of mounts revealed that there were significant differences in the microstructure of the sorbent surfaces, depending on their origin.

Among the agrifood wastes used in this study, the olive mill residue showed the most consistent and firm structure, due to the predominance of olive pits. On the other hand, the artichoke agrowaste SEM images revealed a compact, ordered, and rigid fibril structure with longitudinally arranged fiber cells giving this biomass both toughness and strength [44]. The citrus waste biomass maintained a relatively closely packed structure, displaying a more porous and disintegrated pattern. In all cases, the presence of cavities of irregular shape and dimensions could be appreciated, which would enhance the number of pollutants to be fixed [43,44].
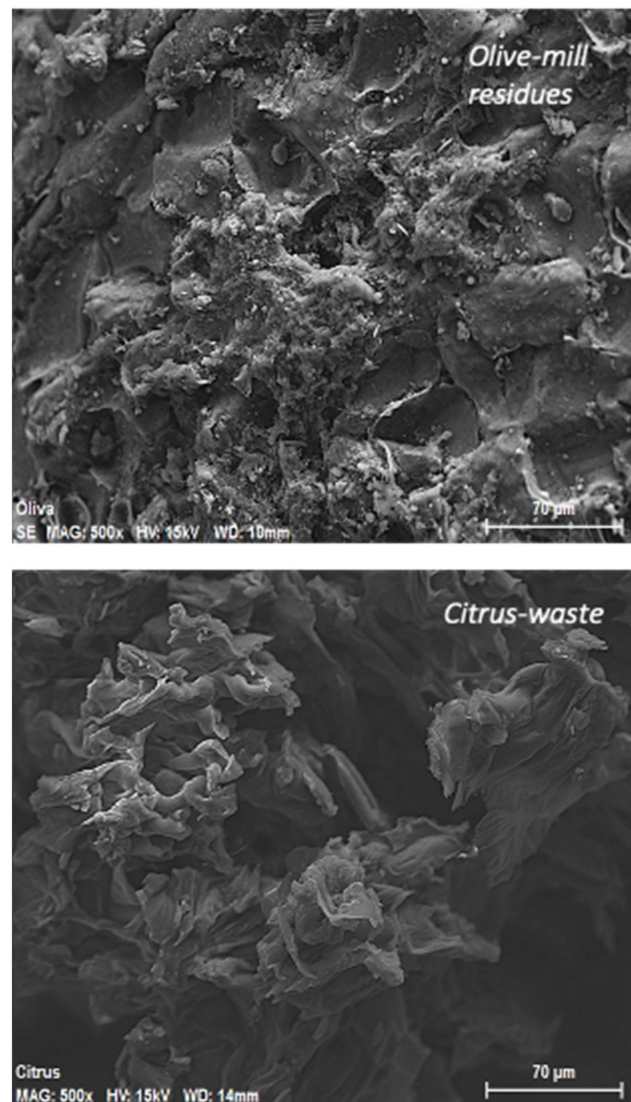

Figure 1. *Cont.*

Figure 1. Scanning electron micrographs of the powder sorbents.

3.3. Crystallinity

Crystallinity is an important feature of plant biomass. It is widely measured and related to the bioconversion of lignocellulose. During cellulose formation, the aggregation of cellulose chains is promoted to form microfibers that can contain two different domains. The crystalline part consists of highly structured cellulose molecules, while the molecules of the amorphous part are less structured. Crystallinity, as expressed by the crystallinity index (*CrI*), was determined from the XRD analysis. The estimation of the *CrI* was made using the empirical Equation (3):

$$CrI\ (\%) = \frac{I_{total} - I_{am}}{I_{total}} \cdot 100 \qquad (3)$$

in which I_{total} is the scattered intensity at the main peaks, whereas I_{am} is the scattered intensity due to the amorphous portion. This parameter (*CrI*) is inversely related to the suitability of the biomass to be hydrolyzed and to the possibility that other molecules may be retained between the cellulose fibers. The olive mill residue showed the highest *CrI* (55.8%), while in citrus waste biomass it was less than 20% (Figure 2). These values are consistent with those previously reported for agrifood residue [13,45,46].
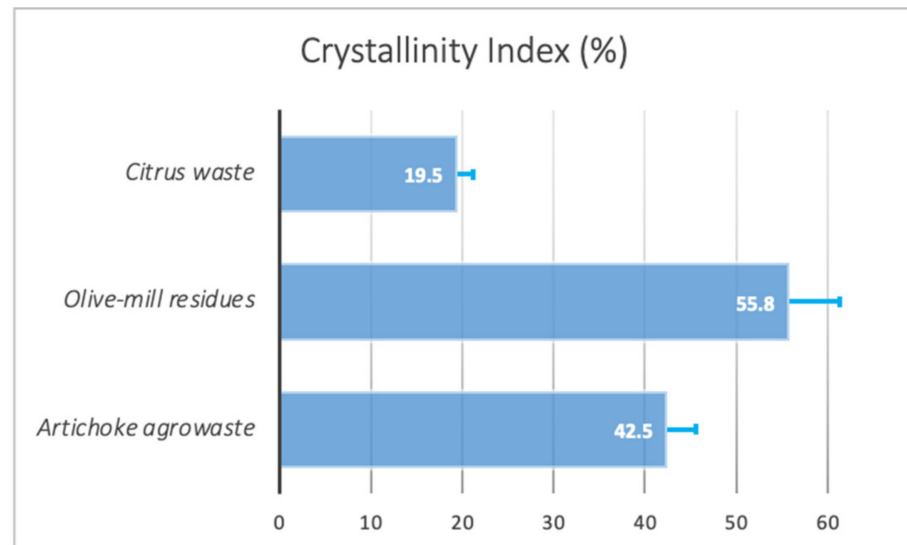
Figure 2. Crystallinity index (mean $\pm$ SD of 3 determinations) of the selected agrifood wastes.

3.4. Fourier-Transform Infrared Spectroscopy

Fourier-transform infrared spectroscopy (FTIR) is an effective tool for determining the surface chemical composition of materials. FTIR spectra offer qualitative and semi-quantitative information suggesting the presence or absence of functional groups in ligno-cellulosic compounds [43]. The FTIR spectra of the selected agrifood wastes are illustrated in Figure 3. All spectra exhibited important intensities in the regions corresponding to 3400 cm^{-1} (peak attributed to the presence of hydrogen-bonded O$-$H, a bond-stretching vibration of α-cellulose), 2900 cm^{-1} (band attributed to the C$-$H stretching of lignocellulosic components, such as CH, CH$_2$, and CH$_3$), 1630 cm^{-1} (due to the presence of carboxyl groups corresponding to the C=O stretching of lignin and the typical skeletal vibrations of aromatic rings), and 1030 cm^{-1} (may be an indication of C$-$O, C=C, and C$-$C$-$O vibrational stretching) [13,47,48]. The main differences between the selected sorbents were in the region of 1200–1400 cm^{-1}.

When comparing the FTIR spectra before and after adsorption, appreciable changes of peak structure (position shifts and intensity change) were observed, which would confirm the involvement of the corresponding groups in the bioremoval process. In general, the most significant changes are shown in the region from 1000 to 1650 cm^{-1}, indicating that lignin functionalities and amino groups participated in the sorption process [47,48].
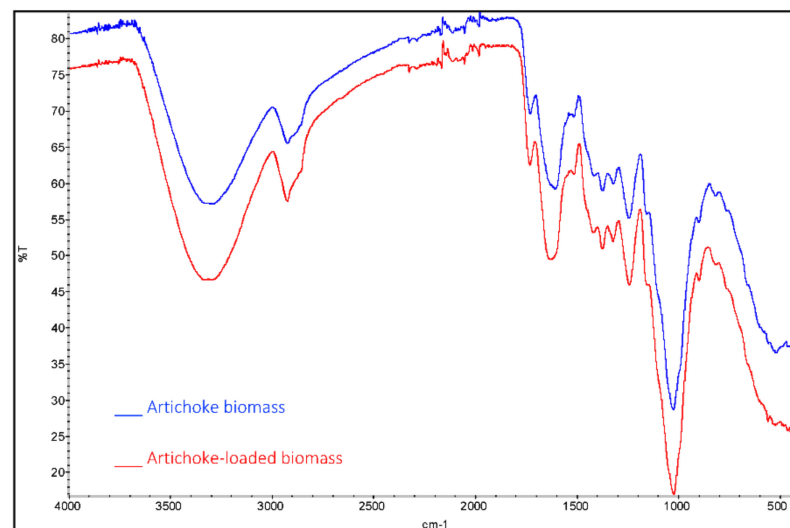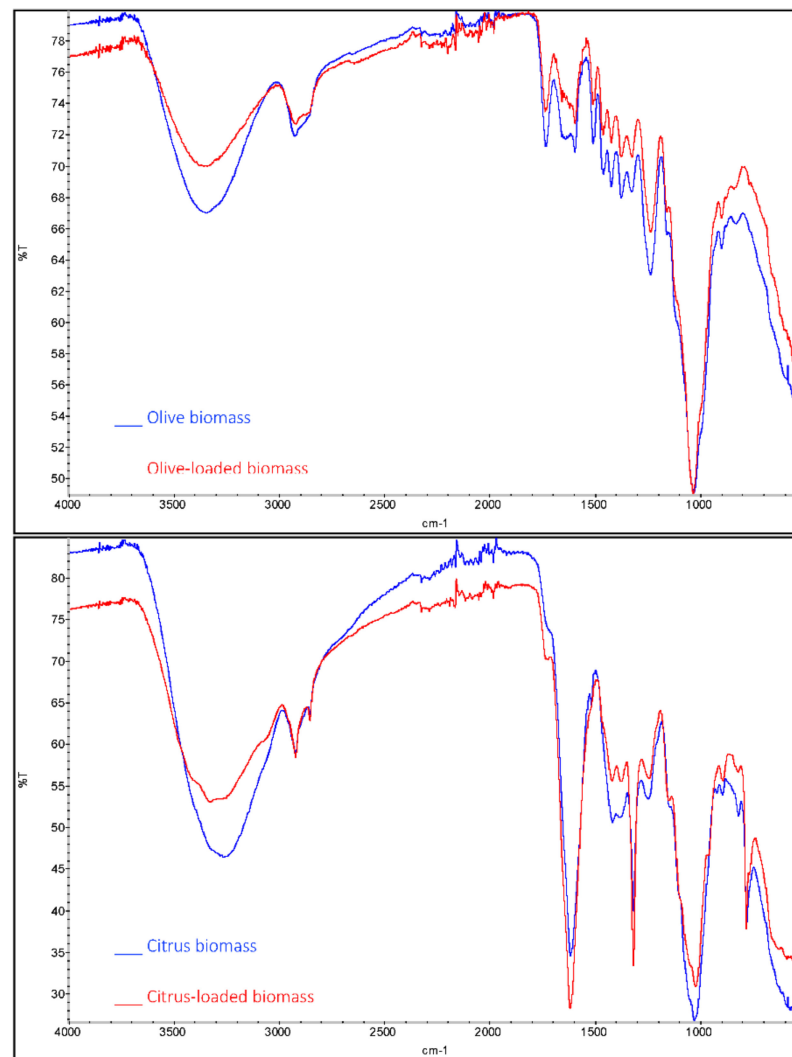

Figure 3. *Cont.*

Figure 3. Fourier-transform infrared spectra of the selected agrifood wastes before and after the sorption process.

3.5. Thermal Analysis

The thermal stability of the selected agrifood residues was investigated using thermogravimetric analysis (TGA) under a N_2 environment. The TGA thermograms are presented in Figure 4. The thermal degradation pattern is ascribed to the inherent structural and chemical characteristics of the agrifood residues which are linked to the presence of lignin, cellulose, and hemicellulose in these biomass samples. The depolymerization of these biopolymers involves dehydration, decarbonylation, decarboxylation, and mainly the cleavage of C−C, C−O, C−H, and glucoside bonds [49]. The thermal degradation data reflects the progressive weight loss which occurred during the heating process, and the first derivative (DTG) reveals the corresponding rate of weight loss. The peak of this graph (DTG$_{max}$) is commonly reported as a value of thermal decomposition and may be used to assess the thermal stability performance of plant residues. It is well established that the thermal decomposition of lignocellulosic plant tissues in an inert atmosphere occurs at mild temperatures for hemicelluloses (250–300 °C), followed by cellulose (300–350 °C), and finally lignin (300–500 °C) [50]. The weight loss curves obtained showed three main decomposition steps. The first mass loss observed was from 25 to 120 °C due to the evaporation of the free water present in the samples, which was much more evident in the artichoke agrowaste and the olive mill residue.
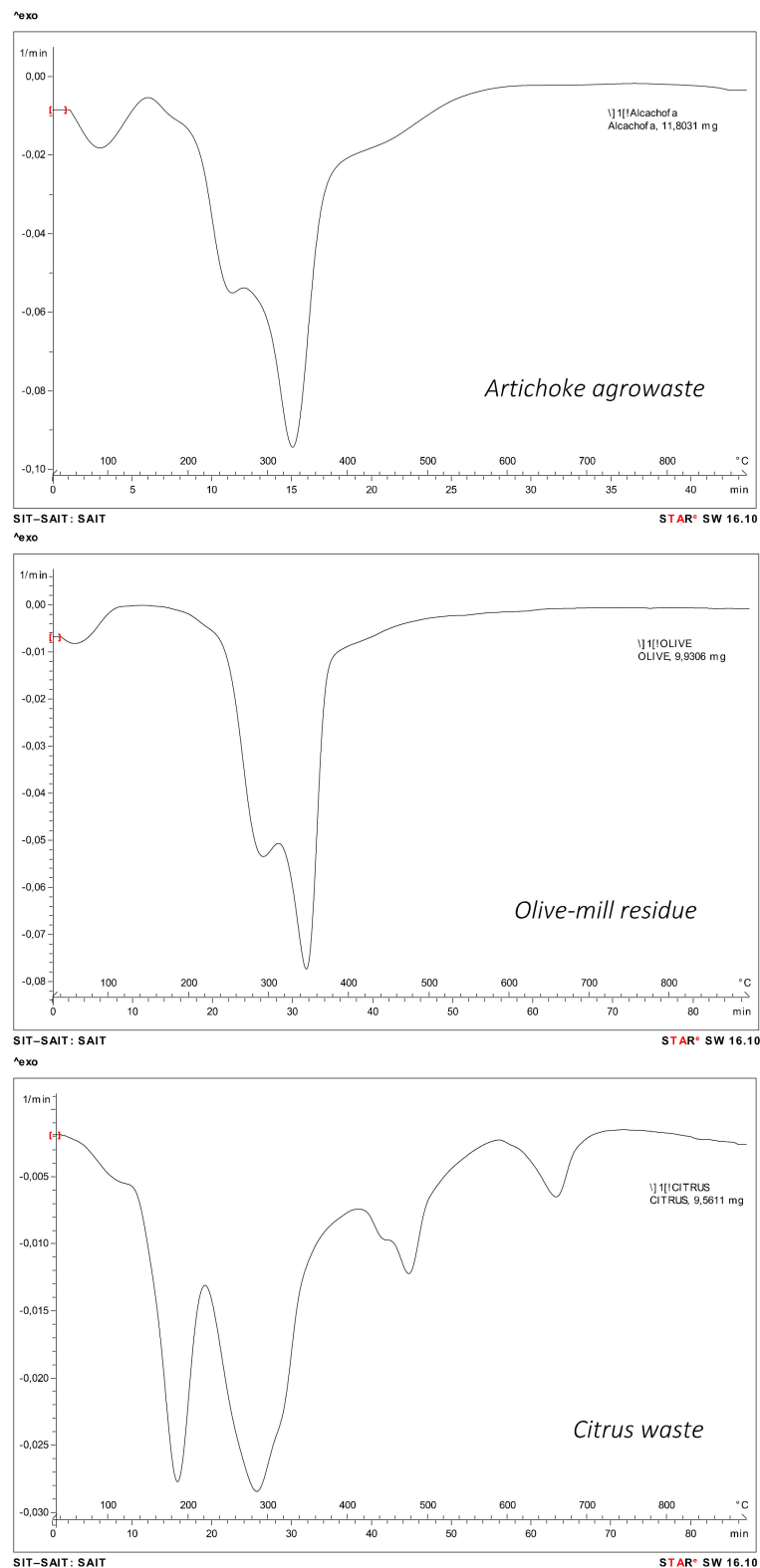
Figure 4. Differential thermogravimetry curves for the selected agrifood wastes.

The weight loss noted around 200 °C was probably caused by the depolymerization and breaking of the hemicellulose bonds, the most thermolabile lignocellulosic components. This phase was particularly prominent in the citrus waste and the artichoke agrowaste. In the third stage (300–375 °C), the cellulose and lignin components and other complex

aromatic structures were decomposed, with only part of the lignin remaining, which is the most complex and resistant component of the biomass [51].

The DTG curves obtained showed that the different agrifood wastes decomposed at a range of temperatures in multi-stage processes with unstable intermediates. The DTG peaks were different in position and height among the samples, implying the specific distribution of organic and inorganic constituents directly affected the thermal decomposition characteristics [49]. The DTG curve corresponding to the citrus waste biomass showed a prominent peak at the temperature of 180 °C, assigned to the presence of pectin, which did not appear in the artichoke agrowaste or the olive mill residue samples.

The resulting values of DTG_{max} ranged from 290 °C (citrus waste) to 340 °C (olive mill residue), with artichoke agrowaste being an in-between value of 337 °C. These results were in good agreement with the values reported in the literature for plant biomass samples [52].

3.6. BET Surface Analysis and Porosimetry

The determination of specific surface areas represents an important concern regarding the characterization of porous and finely dispersed powders. Gas adsorption is the appropriate method to address this concern. If a gas comes into direct contact with a solid material, a portion of the dosed gas molecules is adsorbed onto the surface of this material. The amount of gas adsorbed depends on the gas pressure, the temperature, the kind of gas, and the size of the surface area. After choosing the measuring gas and temperature, the specific surface area of a solid material can be reliably and comparably calculated from the adsorption isotherm. Due to practical reasons, the adsorption of nitrogen at a temperature of 77 K (liquid nitrogen) has been established as the method for the determination of specific surface areas.

Figure 5 shows the sorption isotherms of the three biomass samples and displays the sorption in ultramicropores (<0.7 nm, CO_2 isotherm, Figure 5A), in micropores (<2 nm), and mesopores (2–50 nm) (N_2 isotherm, Figure 5B). It can be seen that the olive mill sorbent is the biomass where the adsorption was most favored. Its nitrogen sorption–desorption isotherm showed hysteresis, which indicates the presence of mesopores. Artichoke agrowaste showed more adsorption in the ultramicropores than in citrus waste; whereas adsorption in micropores was slightly more favored in citrus than in the artichoke agrowaste. The citrus waste also presented hysteresis and thus the presence of mesopores was expected. In the three cases, the strong increase of the adsorbed amount close to the saturation pressure resulted from pore condensation into large meso- and macropores [53]. Total ultramicropore volume was obtained by applying the Dubinin–Radushkevich (DR) method [54]. Interestingly, the citrus waste showed the highest ultramicropore volume (0.066 $cm^3 \cdot g^{-1}$), followed by the olive mill residue (0.038 $cm^3 \cdot g^{-1}$), and the artichoke agrowaste (0.015 $cm^3 \cdot g^{-1}$). The total micropore volume was calculated from the volume of liquid nitrogen adsorbed at $P/P^0 = 0.95$. The values obtained were 0.0019, 0.0048, and 0.0015 $cm^3 \cdot g^{-1}$ for the citrus waste, olive mill residue, and artichoke agrowaste, respectively. Regarding the BET surface area, the olive residue showed the highest value (3.727 $m^2 \cdot g^{-1}$), followed by the citrus waste (1.804 $m^2 \cdot g^{-1}$), and the artichoke agrowaste (0.913 $m^2 \cdot g^{-1}$).

The pore size distributions were obtained using the non-local density functional theory (NLDFT) for the ultramicropore and micropore regions (Figure 6A), and also for the mesopore region (Figure 6B). There are different ways of expressing pore size distributions, but all of them establish the dependence of pore volume on the pore radius or width. In this work, we determined the pore size distribution based on the logarithmic differentiation dV/dlogD. This distribution function reduces the wide apparent disparity of derivative values that the linear distribution of pore sizes dV/dD can create, and is often used in the literature [53]. From the pore size distributions obtained, it can be seen that although there were some mesopores in the three selected residues (Figure 6B), the volume of ultramicropores (Figure 6A) is one order of magnitude higher than that of the mesopores. There were also micropores of 0.8 nm width in the three selected agrifood wastes. From

these figures, it can be easily seen that olive waste was the biomass that exhibited a higher volume of ultra, micro, and mesopores.
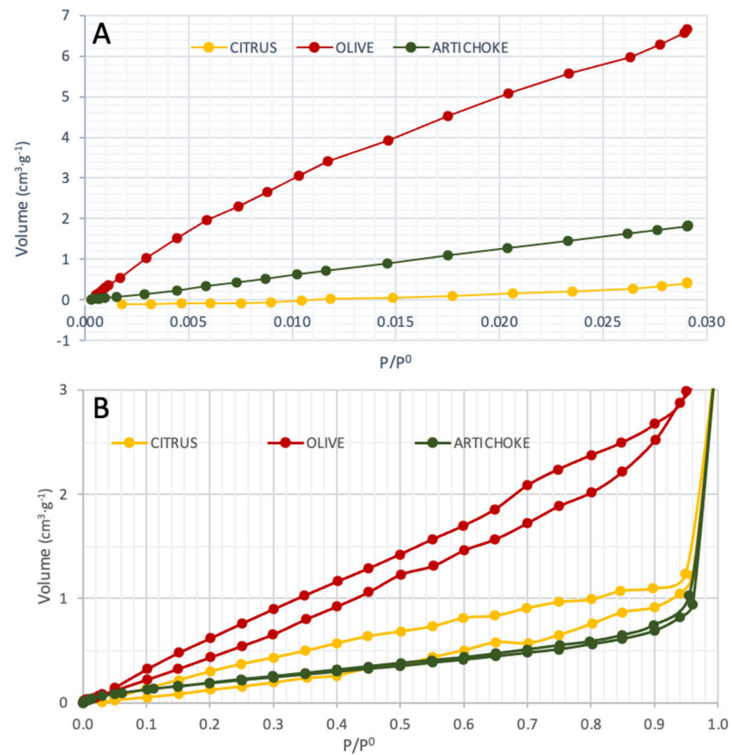

Figure 5. CO_2 (**A**) and N_2 (**B**) sorption isotherms of the artichoke agrowaste, olive mill residue and citrus waste.
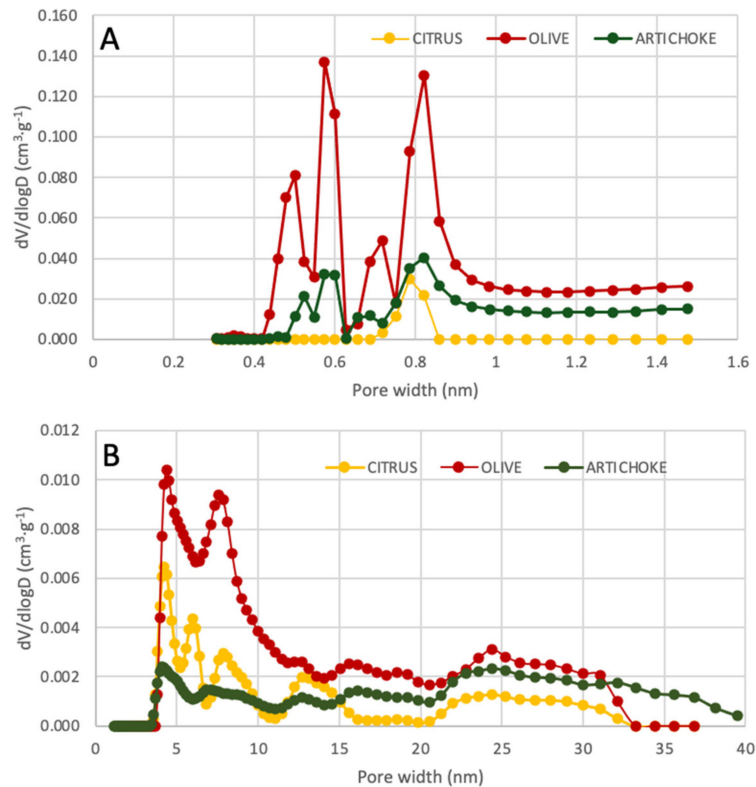

Figure 6. Pore size distribution of the selected agrifood wastes with CO_2 adsorption at 273.15 K (**A**) and with N_2 at 77.3 K (**B**).

Finally, macropore characterization was carried out with Hg porosimetry. The pore size distributions of the macropores are shown in Figure 7. The olive mill residue showed important macropores with an average dimension greater than 75 μm, whereas the citrus waste showed smaller average macropore dimensions of 25 μm. The artichoke agrowaste was the biomass with the lower volume of macropores. However, these findings must be considered with caution given the reported misestimation of porosity and pore size by mercury intrusion when analyzing soft samples [55,56]. In this work, citrus and artichoke biomasses are soft materials with low thickness and their pore walls may break when subjected to mercury porosimetry due to the high working pressures, leading to incorrect results.
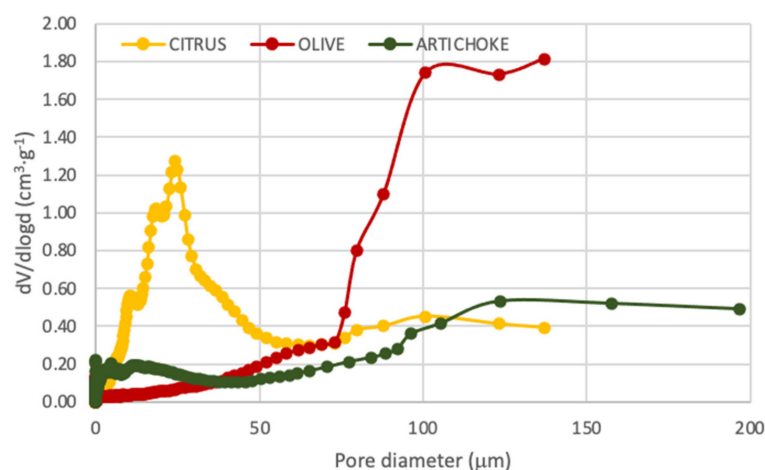

Figure 7. Pore size distribution of macropores in the selected agrifood wastes, performed with Hg porosimetry.

In summary, the surface analysis revealed that olive mill residue showed the highest porosity and BET area, which presumably should translate into a better performance as a sorbent.

3.7. pH of Zero Point of Charge

Sorption processes are numerous, and often do not correspond to simple models. Ion exchange and surface complexation are the main models used to quantify them. The pH of the solution is an important parameter in reactions taking place on particulate surfaces as it controls the surface charge properties of the powder sorbent and must be considered as a target variable to enhance the sorption process [7,39]. Therefore, in the chemical characterization of sorbents, the pH of the zero point of charge (pH_{ZPC}) is one of the key factors to be considered [57].

The pH_{ZPC} for a given sorbent is the pH at which its surface has a net neutral charge, hence it contains as many positively charged as negatively charged surface functions. A given sorbent surface will have a positive charge at solution pH values less than the pH_{ZPC}, and thus will be a surface on which anions may be adsorbed. On the other hand, that sorbent surface will have a negative charge at solution pH values higher than the pH_{ZPC} and thus will be a surface on which positive ions may be adsorbed.

The values of pH_{ZPC} were 4.8, 5.4, and 4.2 for the artichoke agrowaste, olive mill residue, and citrus waste, respectively (Figure 8). In the sorption process, the pH_{ZPC} plays a significant role in the ionization of and interaction between sorbent and sorbates. These values are in the same order of those reported for other raw lignocellulosic biomass samples [39].
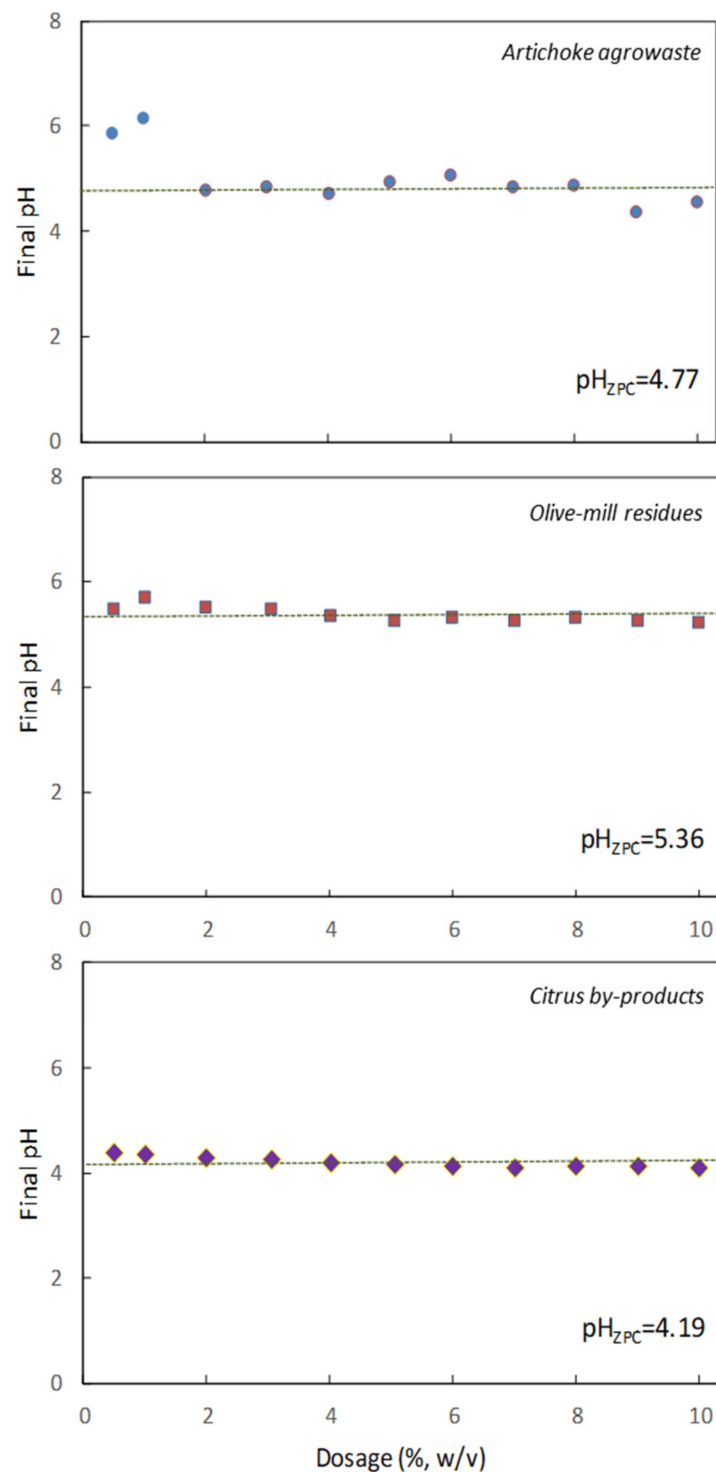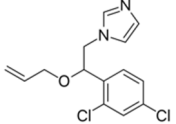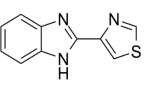
Figure 8. Plots for the pH of zero point of charge determinations.

Because imazalil and thiabendazole are azole biocides (Table 2) with dissociation constants (pK_a) at 25 °C of 6.53 and 4.73, respectively [58], the sorption experiments were conducted at pH 7.0 to achieve a net negative charge on the surface of the powder sorbents and a positive charge around the nitrogen atoms present in the molecules of both biocides, in a way that facilitated electrostatic binding mechanisms to enhance the bioremoval of both pollutants.

Table 2. Sorption capacity (q_e) of the selected agrifood wastes.

	Imazalil (mg·g^{-1})	Thiabendazole (mg·g^{-1})
Artichoke agrowaste	1.9 ± 0.4 *	6.6 ± 1.0
Olive mill residue	9.0 ± 0.8	8.6 ± 0.9
Citrus waste	6.6 ± 0.6	6.1 ± 0.5

* mean ± SD of 3 determinations.

3.8. Imazalil and Thiabendazole Sorption

The agrifood wastes targeted by this research have previously been tested as sorbents to bioremove heavy metals and dyes from aqueous effluent, obtaining excellent results [7–9,11,13,31,59]. However, further research is needed to accomplish the technological development of the results reached at laboratory scale, in addition to examining their performance regarding specific pollutants.

According to results obtained in previous investigations of these sorbents [5,7,13], it was considered beneficial to conduct a prospecting assay to prove the capacity of these lignocellulosic residues to bioremove the biocides IMZ and TBZ present in aqueous effluent. We designed a simple batch experiment at fixed conditions in order to obtain some preliminary results that could inform us about the possibilities of these sorbents to eliminate these contaminants. Table 2 presents the obtained sorption capacity (q_e) values depending on the selected biomass and the biocide tested.

The olive mill residue showed the highest uptake capacity both for IMZ and TBZ, with values of 9.0 and 8.6 mg·g^{-1}, respectively. This represents sorption percentages of 90% (IMZ) and 86% (TBZ) for the olive mill residue. There are few publications reporting on the adsorption of these substances using plant biomass samples. The sorption capacities reported for these biocides with phosphoric acid-activated biomass from *Phoenix canariensis* and its corresponding biochar were between 57–186 mg·g^{-1} [60]. Although it is a fact that the sorption capacities obtained in this investigation are lower than those values reported in the bibliography [58,60], it should be noted that raw agrifood waste is reused without having been subjected to any activation process, either chemical or thermal, and it is well known that carbonaceous materials usually have limited retention capacities. Moreover, the reuse of agrifood wastes would provide additional benefits to the agrifood sector, in parallel to the reduction of pollution from the accumulation of unexploited residues.

Regeneration of the sorbent is an important step in economically checking the feasibility of the sorption process [61]. Desorption assays from the spent sorbents were conducted with NaOH 0.1 M as the eluent agent [62], and the recovery yields ranged from 91.1% (olive mill residue) to 78.4% (citrus waste). The sorbents could be easily regenerated using NaOH eluent and reused for pesticide sorption, suggesting their applicability for water remediation purposes.

4. Conclusions

A commitment must be established to make a more sustainable world, and to this end circularizing waste is mandatory. In recent years, much attention has been given to the reuse of agrifood wastes with a focus on sustainable development and environmental preservation. The large quantity of agrifood waste discarded annually force us to look for alternatives for this interesting feedstock. Thus, food biowaste valorization is one of the imperatives of contemporary society. A strategy for the valorization of typical Mediterranean agrifood wastes as cost-effective sorbents was assessed in order to reduce the ecological footprint of the agrifood sector.

This paper provides comprehensive information on the characterization of the surfaces and the adsorptive properties (SEM, crystallinity, FTIR spectra, TGA, BET surface analysis,

porosimetry, and zero point of charge) of artichoke agrowaste, olive mill residue, and citrus waste, providing evidence that sorption could be a suitable strategy for the effective reuse and recycling of these lignocellulosic residues, in order to promote a zero-waste strategy in these agrifood industries.

Wastewater generated by fruit packaging plants is a critical source of the pollution of natural water resources with biocides such as imazalil or thiabendazole. The adsorption of these biocides onto the agrifood waste-tested samples constitutes a feasible, favorable, and spontaneous process. Low-cost sorption treatment with agrifood waste can reduce the presence of these pollutants in agro-industrial effluent.

References

1. Boto-Álvarez, A.; García-Fernández, R. Implementation of the 2030 agenda sustainable development goals in Spain. *Sustainability* **2020**, *12*, 2546. [CrossRef]
2. Díaz-Sarachaga, J.M.; Jato-Espino, D.; Castro-Fresno, D. Is the sustainable development goals (SDG) index an adequate framework to measure the progress of the 2030 Agenda? *Sustain. Dev.* **2018**, *26*, 663–671. [CrossRef]
3. Lu, Y.; Nakicenovic, N.; Visbeck, M.; Stevance, A.S. Five priorities for the UN sustainable development goals. *Nature* **2015**, *520*, 432–433. [CrossRef]
4. Schwarzenbach, R.P.; Egli, T.; Hofstetter, T.B.; Von Gunten, U.; Wehrli, B. Global water pollution and human health. *Ann. Rev. Environ. Resour.* **2010**, *35*, 109–136. [CrossRef]
5. Rosique, M.; Angosto, J.M.; Guibal, E.; Roca, M.J.; Fernández-López, J.A. Factorial design methodological approach for enhanced cadmium ions bioremoval by Opuntia biomass. *CLEAN Soil Air Water* **2016**, *44*, 959–966. [CrossRef]
6. Yusuf, M.; Elfghi, F.M.; Zaidi, S.A.; Abdullah, E.C.; Khan, M.A. Applications of graphene and its derivatives as an adsorbent for heavy metal and dye removal: A systematic and comprehensive overview. *RSC Adv.* **2015**, *5*, 50392–50420. [CrossRef]
7. Fernández-López, J.A.; Angosto, J.M.; Avilés, M.D. Biosorption of hexavalent chromium from aqueous medium with Opuntia biomass. *Sci. World J.* **2014**, 670249. [CrossRef]
8. Singh, N.B.; Nagpal, G.; Agrawal, S.; Rachna. Water purification by using adsorbents: A review. *Environ. Technol. Innov.* **2018**, *11*, 187–240. [CrossRef]
9. Jahanban-Esfahlan, A.; Jahanban-Esfahlan, R.; Tabibiazar, M.; Roufegarinejad, L.; Amarowicz, R. Recent advances in the use of walnut (*Juglans regia* L.) shell as a valuable plant-based bio-sorbent for the removal of hazardous materials. *RSC Adv.* **2020**, *10*, 7026–7047. [CrossRef]
10. Michalak, I.; Chojnacka, K.; Witek-Krowiak, A. State of the art for the biosorption process—A review. *Appl. Biochem. Biotechnol.* **2013**, *170*, 1389–1416. [CrossRef]
11. Sulyman, M.; Namiesnik, J.; Gierak, A. Low-cost adsorbents derived from agricultural by-products/wastes for enhancing contaminant uptakes from wastewater: A review. *Pol. J. Environ. Stud.* **2017**, *26*, 479–510. [CrossRef]
12. Ncibi, M.C.; Mahjoub, B.; Mahjoub, O.; Sillanpää, M. Remediation of emerging pollutants in contaminated wastewater and aquatic environments: Biomass-based technologies. *CLEAN Soil Air Water* **2017**, *45*, 1700101. [CrossRef]
13. Saavedra, M.I.; Doval Miñarro, M.; Angosto, J.M.; Fernández-López, J.A. Reuse potential of residues of artichoke (*Cynara scolymus* L.) from industrial canning processing as sorbent of heavy metals in multimetallic effluents. *Ind. Crops Prod.* **2019**, *141*, 111751. [CrossRef]

14. Ahorsu, R.; Medina, F.; Constanti, M. Significance and challenges of biomass as a suitable feedstock for bioenergy and biochemical production: A review. *Energies* **2018**, *11*, 3366. [CrossRef]

15. Hu, F.; Ragauskas, A. Pretreatment and lignocellulosic chemistry. *Bioenergy Res.* **2012**, *5*, 1043–1066. [CrossRef]

16. Paul, S.; Dutta, A. Challenges and opportunities of lignocellulosic biomass for anaerobic digestion. *Resour. Conserv. Recycl.* **2018**, *130*, 164–174. [CrossRef]

17. Salem, M.B.; Affes, H.; Ksouda, K.; Dhouibi, R.; Sahnoun, Z.; Hammami, S.; Zeghal, Z.M. Pharmacological studies of artichoke leaf extract and their health benefits. *Plant Foods Hum. Nutr.* **2015**, *70*, 441–453. [CrossRef] [PubMed]

18. Vazquez-Olivo, G.; Gutiérrez-Grijalva, E.P.; Heredia, J.B. Prebiotic compounds from agro-industrial by-products. *J. Food Biochem.* **2019**, *4*, e12711. [CrossRef] [PubMed]

19. Meneses, M.; Megías, M.D.; Madrid, J.; Martínez-Teruel, A.; Hernández, F.; Oliva, J. Evaluation of the phytosanitary, fermentative and nutritive characteristics of the silage made from crude artichoke (*Cynara scolymus* L.) by-product feeding for ruminants. *Small Rumin. Res.* **2007**, *70*, 292–296. [CrossRef]

20. Christoforou, E.; Fokaides, P.A. A review of olive mill solid wastes to energy utilization techniques. *Waste Manag.* **2016**, *49*, 346–363. [CrossRef]

21. Nowicki, P.; Kazmierczak-Razna, J.; Pietrzak, R. Physico-chemical and adsorption properties of carbonaceous sorbents prepared by activation of tropical fruit skins with potassium carbonate. *Mater. Des.* **2016**, *90*, 579–585. [CrossRef]

22. Baruah, J.; Nath, B.K.; Sharma, R.; Kumar, S.; Deka, R.C.; Baruah, D.C.; Kalita, E. Recent trends in the pretreatment of lignocellulosic biomass for value-added products. *Front. Energy Res.* **2018**, *6*, 141. [CrossRef]

23. Menon, V.; Rao, M. Trends in bioconversion of lignocellulose: Biofuels, platform chemicals and biorefinery concept. *Prog. Energy Combust. Sci.* **2012**, *38*, 522–550. [CrossRef]

24. Manna, S.; Toy, D.; Adhikari, B.; Thomas, S.; Das, P. Biomass for water defluoridation and current understanding on biosorption mechanisms: A review. *Environ. Prog. Sustain. Energy* **2018**, *37*, 1560–1572. [CrossRef]

25. Ummartyotin, S.; Pechyen, C. Strategies for development and implementation of bio-based materials as effective renewable resources of energy: A comprehensive review on adsorbent technology. *Renew. Sustain. Energy Rev.* **2016**, *62*, 654–664. [CrossRef]

26. Arief, V.O.; Trilestari, K.; Sunarso, J.; Indraswati, N.; Ismadji, S. Recent progress on biosorption of heavy metals from liquids using low cost biosorbents: Characterization, biosorption parameters and mechanism studies. *CLEAN Soil Air Water* **2008**, *36*, 937–962. [CrossRef]

27. Malik, D.S.; Jain, C.K.; Yadav, A.K. Removal of heavy metals from emerging cellulosic low-cost adsorbents: A review. *Appl. Water Sci.* **2017**, *7*, 2113–2136. [CrossRef]

28. Guidi, P.; Bernardeschi, M.; Palumbo, M.; Genovese, M.; Scarcelli, V.; Fiorati, A.; Riva, L.; Punta, C.; Corsi, I.; Frenzilli, G. Suitability of a cellulose-based nanomaterial for the remediation of heavy metal contaminated freshwaters: A case-study showing the recovery of cadmium induced DNA integrity loss, cell proliferation increase, nuclear morphology and chromosomal alterations on *Dreissena polymorpha*. *Nanomaterials* **2020**, *10*, 1837. [CrossRef]

29. Möller, M.; Schröder, U. Hydrothermal production of furfural from xylose and xylan as model compounds for hemicelluloses. *RSC Adv.* **2013**, *3*, 22253–22260. [CrossRef]

30. Kumar, P.; Barrett, D.M.; Delwiche, M.J.; Stroeve, P. Methods for pretreatment of lignocellulosic biomass for efficient hydrolysis and biofuel production. *Ind. Eng. Chem. Res.* **2009**, *48*, 3713–3729. [CrossRef]

31. Escudero-Oñate, C.; Fiol, N.; Poch, J.; Villaescusa, I. Valorisation of lignocellulosic biomass wastes for the removal of metal ions from aqueous streams: A review. In *Biomass Volume Estimation and Valorization for Energy*; Tumuluru, J.S., Ed.; IntechOpen: Rijeka, Croatia, 2017; pp. 381–407. [CrossRef]

32. Chavan, P.; Singh, A.K.; Kaur, G. Recent progress in the utilization of industrial waste and by-products of citrus fruits: A review. *J. Food Process Eng.* **2018**, *41*, e12895. [CrossRef]

33. Martínez-Patiño, J.C.; Romero, I.; Ruiz, E.; Cara, C.; Romero-García, J.M.; Castro, E. Design and optimization of sulfuric acid pretreatment of extracted olive tree biomass using response surface methodology. *BioResources* **2017**, *12*, 1779–1797. [CrossRef]

34. Machado, M.T.; Eça, K.S.; Vieira, G.S.; Menegalli, F.C.; Martínez, J.; Hubinger, M.D. Prebiotic oligosaccharides from artichoke industrial waste: Evaluation of different extraction methods. *Ind. Crops Prod.* **2015**, *76*, 141–148. [CrossRef]

35. Bollmann, U.E.; Tang, C.; Eriksson, E.; Jönsson, K.; Vollertsen, J.; Bester, K. Biocides in urban wastewater treatment plant influent at dry and wet weather: Concentrations, mass flows and possible sources. *Water Res.* **2014**, *60*, 64–74. [CrossRef] [PubMed]

36. Kahle, M.; Buerge, I.J.; Hauser, A.; Muller, M.D.; Poiger, T. Azole fungicides: Occurrence and fate in wastewater and surface waters. *Environ. Sci. Technol.* **2008**, *42*, 7193–7200. [CrossRef] [PubMed]

37. Channiwala, S.A.; Parikh, P.P. A unified correlation for estimating HHV of solid, liquid and gaseous fuels. *Fuel* **2002**, *81*, 1051–1063. [CrossRef]

38. Sinha, P.; Datar, A.; Jeong, C.; Deng, X.; Chung, Y.G.; Lin, L.C. Surface area determination of porous materials using the Brunauer–Emmett–Teller (BET) method: Limitations and improvements. *J. Phys. Chem. C* **2019**, *123*, 20195–20209. [CrossRef]

39. Fiol, N.; Villaescusa, I. Determination of sorbent point zero charge: Usefulness in sorption studies. *Environ. Chem. Lett.* **2009**, *7*, 79–84. [CrossRef]

40. Fernández-López, J.A.; Castellar, R.; Obón, J.M.; Almela, L. Screening and mass-spectral confirmation of betalains in cactus pears. *Chromatographia* **2002**, *56*, 591–595. [CrossRef]

41. Parikh, J.; Channiwala, S.A.; Ghosal, G.K. A correlation for calculating elemental composition from proximate analysis of biomass materials. *Fuel* **2007**, *86*, 1710–1719. [CrossRef]

42. McKendry, P. Energy production from biomass (part 1): Overview of biomass. *Biores. Technol.* **2002**, *83*, 37–46. [CrossRef]

43. Amiri, H.; Karimi, K. Improvement of acetone, butanol, and ethanol production from woody biomass using organosolv pretreatment. *Bioprocess Biosyst. Eng.* **2015**, *38*, 1959–1972. [CrossRef] [PubMed]

44. Prodromou, M.; Pashalidis, I. Copper (II) removal from aqueous solutions by adsorption on non-treated and chemically modified cactus fibres. *Water Sci. Technol.* **2013**, *68*, 2497–2504. [CrossRef] [PubMed]

45. Rambo, M.K.D.; Ferrerira, M.M.C. Determination of cellulose crystallinity of banana residues using near infrared spectroscopy and multivariate analysis. *J. Braz. Chem. Soc.* **2015**, *26*, 1491–1499. [CrossRef]

46. Mariño, M.; Lopes da Silva, L.; Durán, N.; Tasic, L. Enhanced materials from nature: Nanocellulose from citrus waste. *Molecules* **2015**, *20*, 5908–5923. [CrossRef]

47. Liu, Y.; He, Z.; Uchimiya, M. Comparison of biochar formation from various agricultural by-products using FTIR spectroscopy. *Mod. Appl. Sci.* **2015**, *9*, 246–253. [CrossRef]

48. Wang, F.L.; Li, S.; Sun, Y.X.; Han, H.Y.; Zhang, B.X.; Hu, B.Z.; Gao, Y.F.; Hu, X.M. Ionic liquids as efficient pretreatment solvents for lignocellulosic biomass. *RSC Adv.* **2017**, *7*, 47990–47998. [CrossRef]

49. Manara, P.; Vamvuka, D.; Sfakiotakis, S.; Vanderghem, C.; Richel, A.; Zabaniotou, A. Mediterranean agri-food processing wastes pyrolysis after pre-treatment and recovery of precursor materials: A TGA-based kinetic modeling study. *Food Res. Int.* **2015**, *73*, 44–51. [CrossRef]

50. Carrier, M.; Loppinet-Serani, A.; Denux, D.; Lasnier, J.M.; Ham-Pichavant, F.; Cansell, F.; Aymonier, C. Thermogravimetric analysis as a new method to determine the lignocellulosic composition of biomass. *Biomass Bioenergy* **2011**, *35*, 298–307. [CrossRef]

51. García, A.; Toledano, A.; Serrano, L.; Egüés, I.; González, M.; Marín, F.; Labidi, J. Characterization of lignins obtained by selective precipitation. *Sep. Purif. Technol.* **2009**, *68*, 193–198. [CrossRef]

52. Watkins, D.; Nuruddin, M.; Hosur, M.; Tcherbi-Narteh, A.; Jeelani, S. Extraction and characterization of lignin from different biomass resources. *J. Mater. Res. Technol.* **2015**, *4*, 26–32. [CrossRef]

53. Lowell, S.; Shields, J.E.; Thomas, M.A.; Thommes, M. *Characterization of Porous Solids and Powders: Surface Area, Pore Size and Density*; Springer: Dordrecht, The Netherlands, 2004.

54. Branton, P.; Bradley, R.H. Effects of active carbon pore size distributions on adsorption of toxic organic compounds. *Adsorption* **2011**, *17*, 293–301. [CrossRef]

55. Blacher, S.; Maquet, V.; Pirard, R.; Pirard, J.-P.; Jérôme, R. Image analysis, impedance spectroscopy and mercury porosimetry characterisation of freeze-drying porous materials. *Colloids Surf. A Physicochem. Eng. Asp.* **2001**, *187–188*, 375–383. [CrossRef]

56. Safinia, L.; Mantalaris, A.; Bismarck, A. Nondestructive technique for the characterization of the pore size distribution of soft porous constructs for tissue engineering. *Langmuir* **2006**, *22*, 3235–3242. [CrossRef] [PubMed]

57. Kosmulski, M. The pH dependent surface changing and points of zero charge. VII. Update. *Adv. Colloid Interfaces Sci.* **2018**, *251*, 115–138. [CrossRef] [PubMed]

58. Gamba, M.; Lázaro-Martínez, J.M.; Olivelli, M.S.; Yarza, F.; Vega, D.; Curutchet, G.; Torres Sánchez, R.M. Kinetic and equilibrium adsorption of two post-harvest fungicides onto copper-exchanged montmorillonite: Synergic and antagonistic effects of both fungicides' presence. *Environ. Sci. Pollut. Res.* **2019**, *26*, 2421–2434. [CrossRef]

59. Angosto, J.M.; Roca, M.J.; Fernández-López, J.A. Removal of diclofenac in wastewater using biosorption and advanced oxidation techniques: Comparative results. *Water* **2020**, *12*, 3567. [CrossRef]

60. Martín-González, M.A.; González-Díaz, O.; Susial, P.; Araña, J.; Herrera-Melián, J.A.; Doña-Rodríguez, J.M.; Pérez-Peña, J. Reuse of *Phoenix canariensis* palm frond mulch as biosorbent and as precursor of activated carbons for the adsorption of imazalil in aqueous phase. *Chem. Eng. J.* **2014**, *245*, 348–358. [CrossRef]

61. Chatterjee, A.; Abraham, J. Desorption of heavy metals from metal loaded sorbents and e-wastes: A review. *Biotechnol. Lett.* **2019**, *41*, 319–333. [CrossRef]

62. Hashim, M.A.; Tan, H.N.; Chu, K.H. Immobilized marine algal biomass for multiple cycles of copper adsorption and desorption. *Sep. Purif. Technol.* **2000**, *19*, 39–42. [CrossRef]